THE JOURNAL OF PHYSICAL CHEMISTRY A

Article

pubs.acs.org/JPCA

Electron Transfer in Pnicogen Bonds

Liangyu Guan and Yirong Mo*

Department of Chemistry, Western Michigan University, Kalamazoo, Michigan 49008, United States

Supporting Information

ABSTRACT: As a new type of noncovalent interactions, pnicogen bond between a VA group element (N, P, and As) and an electron donor (Lewis base) has grabbed attention in recent several years. Here we employ the block-localized wave function (BLW) based energy decomposition scheme to probe the bonding nature in a series of substituted phosphines X_nPH_{3-n} complexed with ammonia. As the BLW method can derive the optimal monomer orbitals in a complex with the electron transfer among monomers quenched, we can effectively examine the HOMO−LUMO interaction in these pnicogen bonding systems. Among various energy components, electron transfer energy together with the polarization energy dominates the pnicogen bonding energy. Although usually it is assumed that the electron transfer from ammonia to substituted phosphines occurs in the form of n → σ^*(XP) hyperconjugative interaction, we identify a kind of new pathway when X = NO_2 and CN, i.e., n → dπ^*, which results from the interaction between the π orbital of cyano or nitro substituent and d orbitals on P. But still this picture of electron transfer using a single pair of orbitals is greatly simplified, as the electron density difference (EDD) maps corresponding to the overall electron transfer processes show the accumulation of electron density on the P side opposite to the X−P bond, with insignificant or even negligible gain of electron density on the substituent group side. Thus, the EDD maps tend to support the concept of σ-hole in pnicogen bonds.

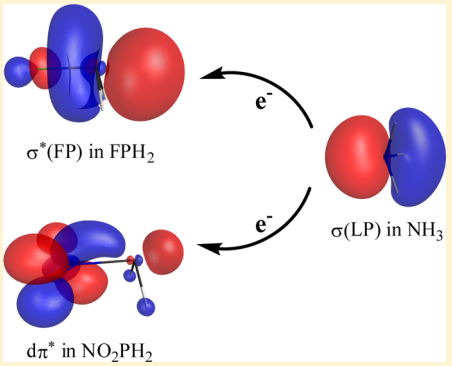

INTRODUCTION

Noncovalent interactions broadly refer to the bonding without the direct involvement of electron sharing between interacting moieties, which can be different molecules or different parts of one molecule, and their magnitude ranges from several (van der Waals, hydrogen bonding) to a couple of dozen kcal/mol (electrostatic and certain strong hydrogen bonding).[1,2] In contrast, a covalent bond results from the sharing of electron pairs between the interacting parts and usually is many times stronger than noncovalent interactions. Even though individual noncovalent interaction is weak and seemingly negligible, the accumulation of many noncovalent interaction leads to a significant force in the formation and function of supermolecules, maintain or folding/unfolding of protein and DNA structures, and rational design of new materials and drugs.[3,4] Some of intermolecular forces such as hydrogen bonding can be highly directional and thus can be applied to the exploration of self-healing rubber-like materials[5] and self-assembling system.[6,7]

Among noncovalent interactions, hydrogen bonding interaction, which widely exists in chemical and biological systems, so far has received the most attention.[8−14] A hydrogen bond A−H···D generally refers to the attractive interaction between the positively charged hydrogen atom and an electronegative atom (such as F, N, or O) or electron-excessive group (such as a π-electron cloud). In other words, hydrogen bonding is predominantly electrostatic in nature,[12,13,15,16] although hyperconjugation (electron transfer) from the donor D to the antibonding orbital of the A−H bond is believed to be also important and responsible for the directionality of the bonding.[17−23] We note that apart from proper hydrogen bonds, where the A−H bond is lengthened and weakened and thus its stretching vibrational frequency is red-shifted, there are also "improper, blue-shifting" hydrogen bonds, where the A−H bond length contracts and thus its stretching mode is blue-shifted, that have been found recently.[24−35]

Apart from hydrogen bond, other types of weak bonds have been identified and explored, including bonds between Lewis bases and VIIA group elements (halogen bond[36−41]), and between Lewis bases and VIA group elements (chalcogen bond[42−47]). Different from hydrogen bonds where a Lewis base approaches the positively charged hydrogen atom, a halogen bond is formed between a Lewis base and a halogen atom. Theoretical analyses revealed that although a halogen atom (A) does not carry partially positive charges, it does have a region of positive electrostatic potential at the head of its lone pair and in the opposite direction of X−A axis. This region is called the "σ-hole",[41,48,49] which can be understood as a crown of positive charge surrounded by a ring of negative charge along the extension of the X−A bond. The existence of σ-holes implies that in halogen bonds, the electrostatic attraction is as directional as the electron transfer interaction. Similarly, VIA group elements can serves as the acceptor of electrons from a

Special Issue: International Conference on Theoretical and High Performance Computational Chemistry Symposium

Received: January 22, 2014
Revised: February 28, 2014
Published: March 3, 2014

   dx.doi.org/10.1021/jp500775m | J. Phys. Chem. A 2014, 118, 8911−8921

Lewis base, resulting in the so-called chalcogen bond. Strong and directional chalcogen−chalcogen interactions or halogen bonds have been explored as connectors in self-assembly systems.[3,6,37,50]

With both halogen and chalcogen bonds confirmed and extensively studied, the possible bonding between a VA group element (N, P, or As, pnictide family) and a Lewis base draws attentions, and this type of weak bond is called pnicogen bond.[51−53] Different from the hydrogen bond but similar to halogen and chalcogen bonds, a pnicogen bond (X)A(H)···D is formed with the electrons transferred from the Lewis base D to the pnicogen atom A, which acts as a Lewis acid and shows a high degree of anisotropy. Here X represents substituent group(s) and H is hydrogen atom(s) bonding to A but not directly interacting with D. For instance, $FPH_2\cdots NH_3$ is a complex where the fluorine atom directs opposite to the N atom with a dihedral angle F−P···N close to 180°. The electron transfer occurs from the lone pair on N to the antibonding orbital σ^*(FP). Hey-Hawkins, Kirchner, Watt, and co-workers first showed the indication of attractive P···P interactions in a $^{13}C\{^1H\}$-NMR spectrum of a *o*-carbaborane derivative and suggested that pnicogen bonds can be used as a molecular linker in complex molecular systems[52,54] and self-assembly processes.[55] Pnicogen bonds involving π systems as Lewis bases also draw interest as the pnicogen−π interaction is relevant in biological systems and plays a role in the protein−substrate bindings.[56] In the past several years, intensive computational studies of pnicogen bonds have been performed, notably by Scheiner and Alkorta et al.[51,53,57−71] It has been known that the strength of a hydrogen bond is related to the electronegativity of the substituted groups bonding to the central atom X. Similarly, the strength of a pnicogen bond is also enhanced as the electronegativity of the substituent X on the electron acceptor A increases; i.e., the pnicogen bonding strength increases in the order X = CH_3 < H < NH_2 < CF_3 < OH < Cl < F < NO_2, and the binding energy in $NO_2PH_2\cdots NH_3$ is close to 7 kcal/mol.[72] Notably, in the $H_2XP\cdots NH_3$ systems, the substituent X positions itself nearly 180° from the nitrogen atom. Other than lone pairs, the π bond system can also serve as electron donors. Several π pnicogen bonds have been investigated, such as $FPH_2\cdots C_2H_4$ where the F−P bond directs to one of the carbon and almost perpendicular to C_2H_4 plane and the H atom is toward to the other carbon.[70]

Whereas all computations confirm the significant stability of pnicogen bonds, which are comparable to the strength of hydrogen bonds, the more intriguing and challenging issue is the elucidation of their bonding nature. Politzer et al. described the $ClH_2P\cdots PH_2Cl$ complex as an example of a double σ-hole interaction.[49] The appearance of σ-holes in pnicogen bonds has also been recognized by others.[73,74] Interestingly, Del Bene et al. studied complexes $H_2C{=}(X)P\cdots PXH_2$ and demonstrated that in the most stable conformations, the pnicogen bonds involve not only π electron donation from $H_2C{=}(X)P$ to PXH_2 through the σ-hole but also donation of the lone pair of PXH_2 to $H_2C{=}(X)P$ through the π-hole.[70] But Scheiner suggested that the attractive electrostatics and charge transfer/induction (polarization) contribute to the pnicogen bonding, and unlike halogen bonds, pnicogen bonds do not require any σ-hole,[58] as the linearity of the X—A···D construct is consistent with the electron transfer from the Lewis base D to the A lobe of the X—A σ^* antibonding orbital.[51] Although electronegative substitutions for a hydrogen atom bonding to the electron acceptor atom strengthen the pnicogen bond, di- or trisubstituion does not produce any additional stabilization. This phenomenon is quite unusual, as more electron-withdrawing groups should increase the acidity of the Lewis bond. This insensitivity to the electron acceptor atom significantly distinguishes the pnicogen bonds from hydrogen bonds.[51]

To probe the various energy contributions to pnicogen bonds and shed new light to the nature of pnicogen bonds, here we employ the block-localized wave function (BLW) method,[75−79] which is the simplest and most efficient variant of ab initio valence bond (VB) methods,[80−83] to analyze the evolution of the interaction between PH_3 and NH_3 with the gradual substitution of hydrogen atoms in PH_3 by various groups. The significance of the BLW method lies in its definition and self-consistent optimization of the hypothetical electron-localized Lewis state where the electron transfer from the Lewis base NH_3 to the Lewis acid PH_3 or its derivatives is strictly turned off. This is achieved by limiting the expansion of one-electron molecular orbitals as having been adopted by many researchers.[84−90]

THEORETICAL METHODOLOGY

It is insightful to interpret intermolecular interactions in terms of a number of physical meaningful energy contributors, though such energy decomposition analyses is far from stringent. Most of the energy decomposition schemes proposed so far fall in the category of the supermolecular method,[16,91−100] where a supermolecule is composed of *M* monomers;the total binding energy (ΔE_b) is defined as the energy change from isolated monomers to the supermolecule,

$$\Delta E_b = E_{Super} - \sum_{i=1}^{k} E_{Mono}(i) \quad (1)$$

Compared with other energy decomposition approaches, the block-localized wave function (BLW) method is unique as it can define the electron-localized state where the energy transfer among monomers are strictly deactivated and whose wave function can be self-consistently optimized.[75−77] The fundamental assumption in the BLW method is that the total electrons and primitive basis functions can be divided into a few subgroups (blocks), and each subgroup corresponds to a monomer in the current study of intermolecular interactions. Molecular orbitals are block-localized, in other words, they are expanded in only one subgroup of basis functions. Orbitals in the same subgroup are constrained to be orthogonal, but orbitals belonging to different subspaces are nonorthogonal. The final electron-localized state wave function is expressed with one Slater determinant. Thus, the BLW method combines the advantages of both MO and VB theories. The BLW method has been extended to the DFT level.[77]

With the definition of electron-localized state, the intermolecular interaction can be interpreted in a few successive steps.[78,79] First, monomers experience unfavorable geometry deformations from their respective free and optimal states to the distorted geometries in the optimal structure of the supermolecule, and the energy change in this step is defined as the deformation energy (ΔE_{def}). Second, the distorted monomers are brought together to form the supermolecule without further perturbing the structures of monomers, and all monomer electron densities are frozen and there is even no electron exchange among monomers. Energy variation thus corresponds to the classical electrostatic energy (ΔE_{ele}). Third, the electron exchange among monomers is allowed by

dx.doi.org/10.1021/jp500775m | J. Phys. Chem. A 2014, 118, 8911−8921

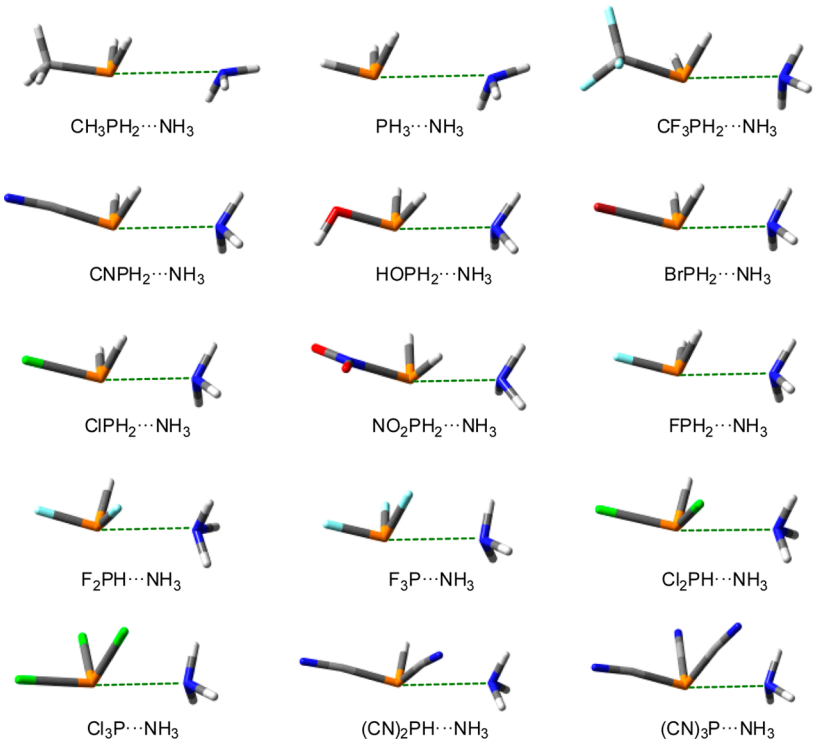

Figure 1. Optimal geometries with green dashed lines showing pnicogen bonds.

imposing the antisymmetrization on the previous Hartree product. The subsequent energy change (ΔE_{ex}) results from the quantum Pauli exchange. We note that the definitions of the electrostatic and exchange energies are similar to those in the Kitaura–Morokuma analysis[91] and the extended transition state (ETS) based energy decomposition analysis.[101−103] Due to the difficulty in the computation of the exchange energy within the DFT theory, we often combine the electrostatic and Pauli exchange interactions together and call the energy change as the quasi-Heitler–London energy (ΔE_{qHL}). The fourth step is the redistribution of electron density within each monomer due to the electric field imposed by the other monomers. This is an energy-lowering step for the complex and the resulting energy change is called polarization energy (ΔE_{pol}). Note that at this stage the state wave function is the optimal BLW. Finally, we allow electrons to delocalize among monomers, and get the final state of this supermolecule. The stabilization energy in this step is defined as the charge transfer energy (ΔE_{ct}). As such, we decompose the overall intermolecular interaction energy into a set of physically meaningful contributions as

$$\Delta E_b = \Delta E_{def} + \Delta E_{qHL} + \Delta E_{pol} + \Delta E_{ct} \quad (2)$$

Additional electron correlation energy term (ΔE_c) can be defined which highlights the binding energy difference at a higher theoretical level compared with a lower theoretical level. The definition of a separate term for electron correlation is supported by our recent work on the use of density-dependent dispersion correction in the energy decomposition analyses, which show that both the polarization and charge transfer energies are little affected by the inclusion of the electron correlation.[104]

COMPUTATIONAL DETAILS

We studied the pnicogen bonds in a series of $X_nPH_{3-n}\cdots NH_3$ complexes. Geometry optimizations were performed at the MP2/aug-cc-pVDZ level of theory and shown in Figure 1 (details see the Supporting Information). The subsequent BLW energy decomposition analyses were conducted with our in-house version of the quantum mechanical software GAMESS at the DFT(wB97x-D)/cc-pVTZ level,[105] where Grimme's dispersion correction[106] is applied and the change of dispersion energy (or correlation energy ΔE_c in general) is calculated as

$$\Delta E_c = E_{disp}^{DFT} - \sum_{i=1}^{k} E_{disp}^{i} \quad (3)$$

where E_{disp}^{DFT} is the dispersion correction energy of the final complex and E_{disp}^{i} is the dispersion correction energy of each distorted monomer.

RESULTS AND DISCUSSION

Orbital Correlation Diagram Based on the BLW Computations. One fundamental and widely adopted theoretical tool in the prediction and interpretation of chemical reactions is the orbital interaction (or correlation) diagram, where the interacting orbitals of reactants and product are linked. By observing the shifting of energy levels of frontier orbitals, we can elucidate the reaction pathways and identify the direction of electron movement. Usually an orbital correlation diagram is made on the basis of the separate computations of reactant molecules and product molecule(s). But this may cause a potential problem as the orbital energy levels of a molecule will change simply in the presence of another molecule even before any chemical reaction (i.e., electron movements among reactants) occurs. For the current study of the intermolecular interaction between a Lewis acid and a Lewis base, the energy levels of a monomer are certainly

dx.doi.org/10.1021/jp500775m | J. Phys. Chem. A 2014, 118, 8911−8921

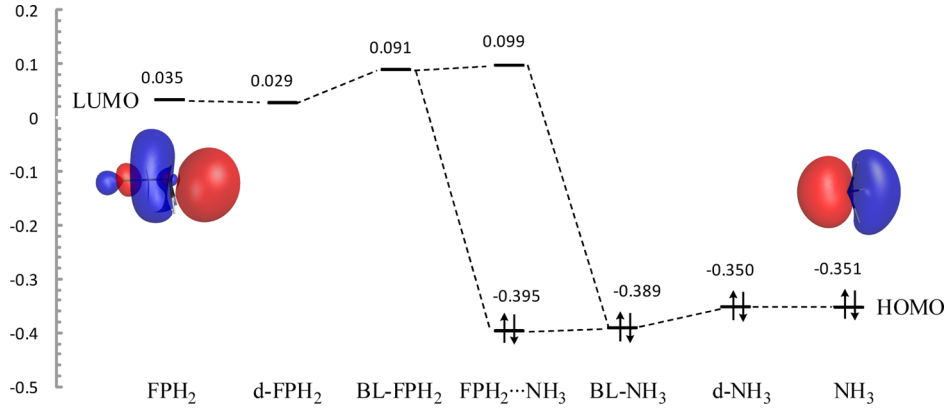

Figure 2. Molecular orbital energy change (in hartree) and the orbital correlation diagram in the formation of the $FPH_2\cdots NH_3$ complex, where d and BL denote the deformed and block-localized monomers at the geometry of the optimal complex.

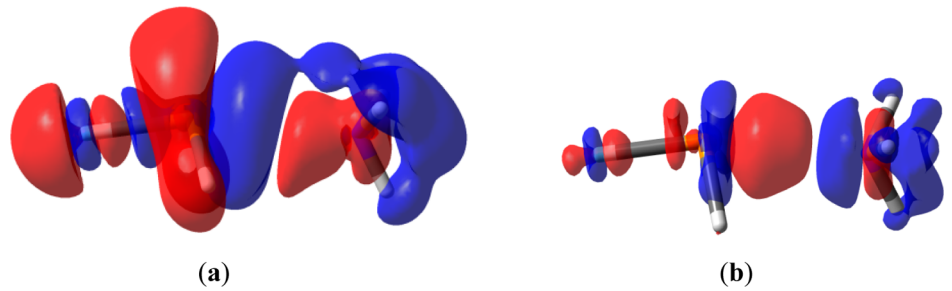

Figure 3. Electron density difference maps showing (a) polarization and (b) electron transfer in the $FPH_2\cdots NH_3$ complex (contour isodensity value 0.0004 au). Red/blue colors refer to the gain/loss of electron densities.

different when it is isolated or it is coupled with another monomer. The advantage of the BLW method is that we can probe the orbital energy changes in a monomer due to the presence of another monomer, when the electron transfer between monomers is quenched. The subsequent in situ orbital correlation diagram can give us a better idea regarding the interaction between the HOMO and LUMO.

Here we examine the evolution of the orbital energies in the $FPH_2\cdots NH_3$ complex. The computations of individual optimal monomers show the compatibility of the HOMO of NH_3 and the LUMO of FPH_2 as shown in Figure 2 with an energy gap 0.386 au (10.50 eV). The structural deformation to the geometries in the optimal complex changes the energy levels slightly. However, when the two monomers approach, considerable shifting of orbital energy levels is observed. This can be well understood as the effect from the electrostatic field of another monomer as well as the associated rearrangement of the electron densities within monomers. We observe the destabilization of the LUMO of FPH_2 and the stabilization of the HOMO of NH_3, and as a consequence, the HOMO−LUMO energy gap increases to 0.480 au (13.06 eV). This represents an increase of 2.56 eV (26.6%) from the gap from separated monomers. Finally, the electron flow from the HOMO to the LUMO stabilizes the former but destabilizes the latter. Though it seems that the magnitudes of these changes are rather limited, i.e., by 0.16 eV for the HOMO and 0.22 eV for the LUMO, we can estimate that there is 2×0.16 eV = 7.48 kcal/mol stabilization energy from the HOMO−LUMO or the $n \rightarrow \sigma^*(FP)$ hyperconjugative interaction in the $FPH_2\cdots NH_3$ complex, if the repulsion within the electron pair is not counted. A more complete energy decomposition analysis confirms that the electron transfer stabilization is 4.87 kcal/mol (see the following section). Still, this value is impressive for noncovalent interactions (e.g., the total binding energy in $FPH_2\cdots NH_3$ is 6.37 kcal/mol), though it is dramatically different from the NBO result (18.18 kcal/mol), which is almost 3 times the binding energy between FPH_2 and NH_3.[72] If we start from the energy levels from separated monomers as shown in Figure 2, we would see the significant HOMO−LUMO interactions and expect much exaggerated electron transfer interaction.

The orbital energy level shifts can be partially visualized and understood with the electron density difference (EDD) maps. The EDD between the optimal BLW and the sum of individual monomers (i.e., the initial BLW) in the complex reflects the redistribution of the electron density within each monomer due to the influence of the other, i.e., the polarization effect, whereas the difference between the regular DFT and BLW electron densities corresponds to the electron transfer between the two monomers. Obviously, both the polarization and electron transfer shifts the energy levels as exhibited in Figure 2. Parts a and b of Figure 3 show the EDD maps of $FPH_2\cdots NH_3$ due to the polarization effect and electron transfer, respectively. Note that unlike the orbital plots shown in Figure 2 where the red and blue colors mean the different phases of orbitals, here in EDD maps the blue color represents a loss and the red refers to a gain of electron density. With the approaching of NH_3 to FPH_2, electron density shifts from hydrogen atoms to the nitrogen atom. This shift enhances the density of the nitrogen lone pair area along the P direction and prepare for the subsequent electron transfer. In contrast, the electron density in FPH_2 polarizes away from the phosphorus atom side and this redistribution vacates the space along the Lewis base side in preparation for the acceptance of electron from NH_3. Due to

dx.doi.org/10.1021/jp500775m | J. Phys. Chem. A 2014, 118, 8911−8921

Table 1. BLW Energy Decomposition Analysis of the Binding between a Monosubstituted Phosphine and Ammonia (kcal/mol) and the optimal P···N Distance (Å)

phosphine	ΔE_{def}	ΔE_{HL}	ΔE_{pol}	ΔE_{ct}	ΔE_{c}	ΔE_{b}	R_{PN}
CH_3PH_2	0.01	−0.13	−0.24	−0.39	−0.72	−1.47	3.320
PH_3	0.03	−0.32	−0.27	−0.40	−0.67	−1.63	3.302
CF_3PH_2	0.28	−1.30	−0.91	−1.14	−0.80	−3.88	3.034
$CNPH_2$	0.26	−2.06	−1.06	−1.33	−0.81	−5.00	2.988
$HOPH_2$	0.49	−0.23	−1.19	−1.95	−0.85	−3.74	2.870
$BrPH_2$	0.79	1.11	−2.33	−4.07	−0.93	−5.45	2.709
$ClPH_2$	0.93	0.78	−2.34	−4.18	−0.92	−5.73	2.694
NO_2PH_2	0.85	0.48	−3.05	−4.94	−0.94	−7.60	2.645
FPH_2	1.13	0.91	−2.62	−4.87	−0.92	−6.37	2.624

the collective electrostatic and polarization interactions, we observe the upshifting of the LUMO of FPH_2 and the downshifting of the HOMO of NH_3. The electron transfer, as shown in Figure 3b and in accord with our presumption, shifts the electron density from the nitrogen atom side to the phosphorus atom side and further enhances the HOMO−LUMO energy gap, though the magnitude is very small. If we combine both EDD maps together, the usual n → σ*(FP) description is very approximate as it implies that only one single pair of orbitals is involved, as Scheiner pointed out.[66] Figure 3b clearly shows that all three hydrogen atoms in NH_3 make contributions to the electron transfer to FPH_2.

Pnicogen Bonds between Ammonia and Monosubstituted Phosphines. Similarly to the work by Scheiner,[72] we studied the interaction of NH_3 with a series of monosubstituted phosphines XPH_2, with X = CH_3, OH, CF_3, CN, Br, Cl, F, and NO_2. Table 1 compiles the P···N distances at their optimal complex geometries and the binding energies with contributing energy components. The deformation energy costs are essentially from the phosphines, as in all complexes the deformation penalty for ammonia is no more than 0.01 kcal/mol. Our binding energies are also comparable to the results at the CCSD(T)/aug-cc-pVTZ theoretical level.[66]

There is a good correlation between the binding energies and bond distances,[72] as the binding energy increases (in absolute values) linearly with the decreasing bond length (shown in Figure 4). This is also in accord with the increasing electronegativity of the substituent. However, Figure 4 shows that there are three phosphines are notably away from the linear correlation, i.e., X = OH, CN, and NO_2. Among these three outliers, phosphinous acid (X = OH) has a binding energy lower than the value suggested by the regression line in the formation of a pnicogen bond with ammonia. In contrast, both phosphinous cyanide (X = CN) and nitrophosphine (X = NO_2) have higher binding energies than predicted. These deviations suggest the possibly different binding patterns in these systems from those abiding by the regression line.

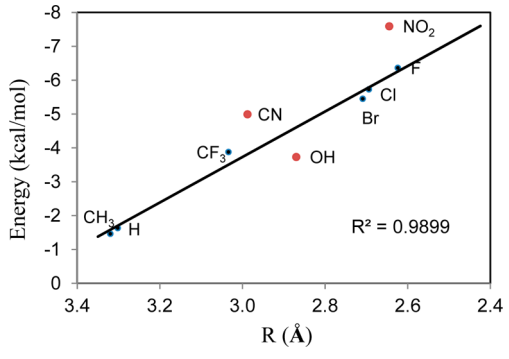

Figure 4. Correlation between bond length and binding energy between monosubstituted phosphines and ammonia.

For phosphinous acid, if we compare it with two neighboring systems in Figure 4 that follow the regression line, i.e., X = CF_3 and Br, and examine their energy components in Table 1, we see that each energy term for phosphinous acid is in the middle of the values for (trifluoromethyl)phosphine and phosphinous bromide except the charge transfer energy term, which is remarkably below the middle point. We further check the HOMO and LUMO energy levels and the corresponding gap, as listed in Table 2. The HOMO−LUMO gap in the electron-localized diabatic state for phosphinous acid is high (12.46 eV) and very close to the gap in (trifluoromethyl)phosphine (12.52 eV), leading to the poorer electron transfer capability than expected. The likely reason is the intramolecular hydrogen bonding in phosphinous acid as shown in Figure 5. This intramolecular hydrogen bond reduces the bonding capability of phosphorus with ammonia.

Table 2. Orbital Energies of the HOMO and LUMO (hartree) and the HOMO−LUMO Gaps (eV) for the Complexes of Monosubstituted Phosphines with Ammonia

	BLW			DFT		
phosphine	HOMO	LUMO	gap	HOMO	LUMO	gap
CH_3PH_2	−0.350	0.090	11.97	−0.352	0.090	12.03
PH_3	−0.354	0.107	12.54	−0.359	0.096	12.38
CF_3PH_2	−0.376	0.084	12.52	−0.384	0.081	12.65
$CNPH_2$	−0.384	0.069	12.33	−0.388	0.077	12.65
$HOPH_2$	−0.370	0.088	12.46	−0.376	0.083	12.49
$BrPH_2$	−0.387	0.045	11.76	−0.409	0.043	12.30
$ClPH_2$	−0.388	0.063	12.27	−0.417	0.069	13.22
NO_2PH_2	−0.402	0.007	11.13	−0.422	0.012	11.81
FPH_2	−0.389	0.091	13.06	−0.395	0.099	13.44

For the interaction between nitrophosphine and ammonia, Table 1 shows that the abnormally high binding energy is largely due to the high electron transfer stabilization, which is the highest among the monosubstituted phosphines studied in this work. Although this is in accord with its HOMO−LUMO

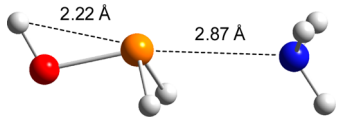

Figure 5. Geometry of the $HOPH_2$···NH_3 complex.

dx.doi.org/10.1021/jp500775m | J. Phys. Chem. A 2014, 118, 8911−8921

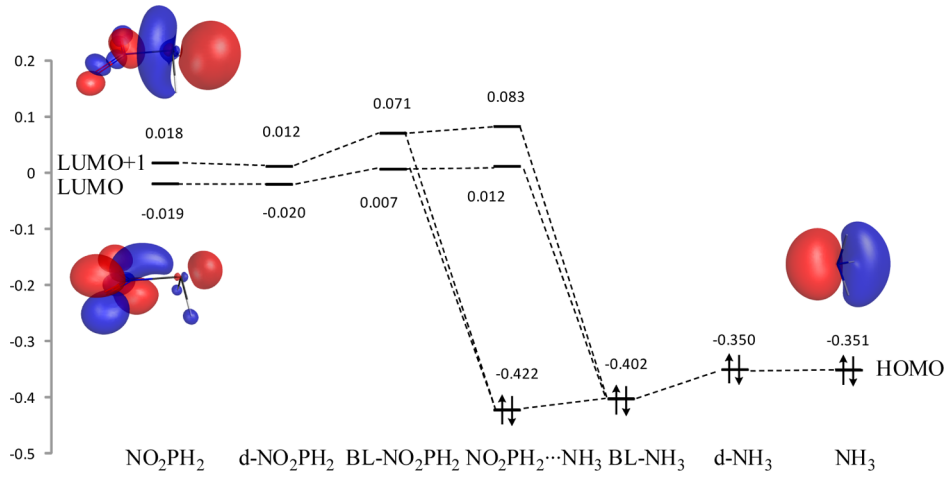

Figure 6. Molecular orbital energy change (in hartree) and the orbital correlation diagram in the formation of the $NO_2PH_2\cdots NH_3$ complex, where d and BL denote the deformed and block-localized monomers at the geometries of the optimal complex.

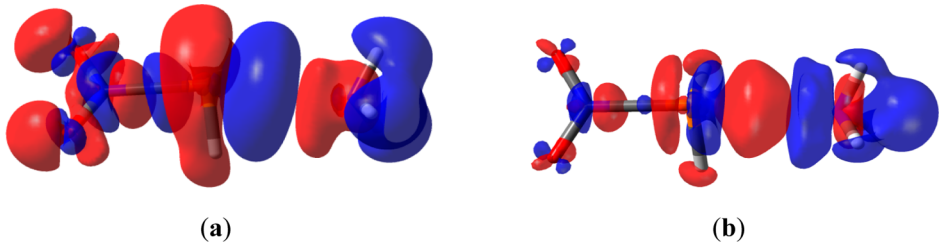

Figure 7. Electron density difference maps showing (a) polarization and (b) electron transfer in the $NO_2PH_2\cdots NH_3$ complex (contour isodensity value 0.0004 au). Red/blue colors refer to the gain/loss of electron densities.

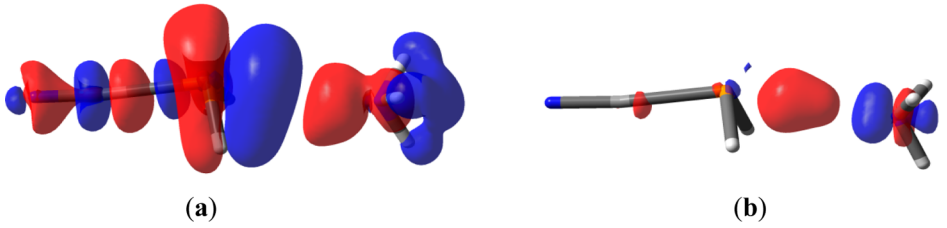

Figure 8. Electron density difference maps showing (a) polarization and (b) electron transfer in the $CNPH_2\cdots NH_3$ complex (contour isodensity value 0.0004 au). Red/blue colors refer to the gain/loss of electron densities.

gap that is the lowest in Table 2, a detailed look of orbital interactions reveals that apart from the regular n → σ^*(NP) hyperconjugative interaction, there is also electron transfer interaction from the lone pair on the nitrogen of ammonia to a dπ^* orbital that forms from the strong interaction between the π orbital on the nitro group and the vacant d atomic orbital on P. As a matter of fact, this dπ^* orbital has a lower energy than σ^*(NP) and thus is the LUMO, whereas σ^*(NP) is the LUMO +1. For comparison, in the complex $FPH_2\cdots NH_3$, the LUMO is σ^*(FP). Figure 6 shows the orbital correlation in $NO_2PH_2\cdots NH_3$ where both the LUMO and LUMO+1 are plotted. With the approach of ammonia, both the LUMO and LUMO+1 lift their energy levels due to the electrostatic field of NH_3, but the latter increases its energy level more than the former. Both participate in the interaction with the HOMO of NH_3, but we can expect that the dπ^* orbital is more effective in interactions and accepts more electrons than σ^*(FP). Parts a and b of Figure 7 show the EDD maps of $NO_2PH_2\cdots NH_3$ due to the polarization effect and electron transfer, respectively. The patterns of polarization and electron transfer are very similar to those in $FPH_2\cdots NH_3$ (Figure 3). The electron density within NH_3 polarizes from three hydrogen atoms to the p orbital along the P direction, whereas the electron density in NO_2PH_2 polarizes away from the phosphorus atom side. The subsequent electron transfer can be described as n → σ^*(NP) hyperconjugation. But compared with the orbital diagrams in Figure 6, the nitro group side gains much less electron density than expected. Alternatively, similar to Figure 3b, Figure 7b is consistent with the concept of σ-hole on P.

Similar to the case for nitrophosphine, the LUMO of phosphinous cyanide is the dπ^* orbital as well due to the electron delocalization of the π electron pairs on the cyano group to the vacant d orbitals on P. The energy level of the LUMO in $CNPH_2\cdots NH_3$ is higher than that in $NO_2PH_2\cdots NH_3$, leading to low electron transfer stabilization energy. Interestingly, Table 1 shows that the much higher binding energy $CNPH_2\cdots NH_3$ is notably contributed by the quasi-Heitler−London energy, which is composed of the repulsive Pauli exchange energy and the electrostatic interaction. In other words, there is considerable electrostatic attraction between

dx.doi.org/10.1021/jp500775m | J. Phys. Chem. A 2014, 118, 8911−8921

$CNPH_2$ and NH_3, which results in the abnormally high binding energy. In $CNPH_2\cdots NH_3$, the charge transfer energy is similar to that in $FPH_2\cdots NH_3$, so is the polarization effect. Parts a and b of Figure 8 plot the EDD maps for the polarization and electron transfer effects. We note that in this case, the electron transfer pattern better be described as from the lone pair on nitrogen to the σ-hole on P rather than to the antibonding orbital σ^*(NP), which would have a significant portion on the nitrogen atom side. The existence of σ-hole is also consistent with the high electrostatic attraction.

The significant finding by the general survey of all complexes studied here, however, is that the binding energy is dominated by the stabilizing polarization and electron transfer contributions, particularly when the substituent groups are of high electronegativity. Table 1 shows that when X = Br, Cl, F, and NO_2, the charge transfer energy is over 4 kcal/mol and accounts for more than half of the total binding energies. The high stabilization, further supplemented by the polarization effect, shortens the P···N distance at the expense of the repulsive quasi-Heitler–London energy (more precisely, the Pauli exchange energy) and the deformation cost. The EDD maps for the electron transfer in these systems, however, seem to support the existence of σ-hole in monosubstituted phosphines, as the gain of electron density is mostly concentrated on the P side opposite to the X–P bond.

To further look into the correlation between the charge transfer energy and the pnicogen bond distance, we plotted Figure 9. It has been known that the rate of electron transfer

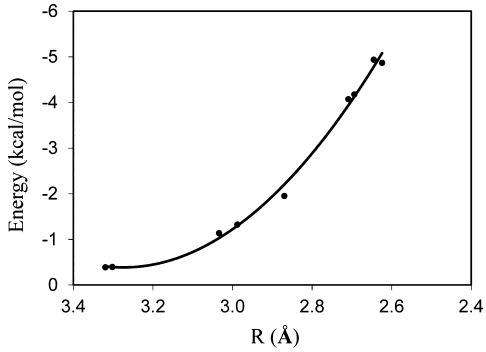

Figure 9. Correlation between bond length and electron transfer stabilization energy between monosubstituted phosphines and ammonia.

decreases exponentially with the distance.[107] Using the BLW method, previously we also demonstrated the exponential correlation between the electronic coupling energy and the donor–acceptor distance.[108,109] Similarly, Figure 9 shows that the electron transfer energy increases exponentially with the shortening of the pnicogen bond.

Pnicogen Bonds between Ammonia and Multisubstituted Phosphines. We studied the interactions of multisubstituted X_nPH_{3-n} (n = 1–3, X = F, Cl, and CN) with NH_3, and Table 3 compiles the optimal pnicogen bond distances and binding energies with decomposed components. Similar to the monosubstituted phosphines, multisubstituted phosphines are almost fully responsible for the deformation energy costs as the deformation energy for ammonia is less than 0.04 kcal/mol.

In the previous section, we show that for monosubstituted phosphines, the electron-withdrawing substituent could increase the interaction of XPH_2 with Lewis bases. This is understandable as the more electronegative the substituent is, the larger is the weight of the antibonding σ^*(XP) orbital on the phosphorus (or, the more positive is the σ-hole[48]). The larger portion of σ^*(XP) on P results in a better overlap with the donating monomer and thus accepts more electron density from the Lewis base. Alternatively, the increased positiveness of the σ-hole enhances the electrostatic attraction with the Lewis base. Figure 4 shows the increasing binding energy with the increasing electronegativity from lower left to upper right. Following this trend, we may expect that multisubstitution with electron-withdrawing substituents would further strengthen the pnicogen bond. However, Table 3 demonstrated that this is not necessarily the case. For multihalogenations (X = F, Cl), the pnicogen bond is actually weakened. Our energy decomposition analyses indicate that the bond strength is determined by a variety of factors, not only the orbital interaction. Though multisubstitution does increase the polarity of the X–P bond (or, within the σ-hole theory increases the attraction of the σ-hole to the Lewis donor) and reversely polarizes the σ^*(XP) toward the P side and subsequently increases the electron transfer interaction, as evidenced by the decreasing HOMO–LUMO gap listed in Table 4, there are also the deformation cost for the phosphine and the Pauli repulsion between the phosphine and ammonia that tend to oppose the approach of the two species. As a compromise, we see the lengthening of the pnicogen bond with the gradual substitution of hydrogen by halogen atoms.

Interestingly, the cyano group has a strikingly different performance from the halogen atoms, and the multisubstitution by cyano groups significantly enhances the pnicogen bond, with $(CN)_3P\cdots NH_3$ having the largest binding energy and the shortest P···N distance. Considering the abnormal behavior of $CNPH_2$ among monosubstituted phosphines (Figure 4), which

Table 3. BLW Energy Decomposition Analysis of the Binding between a Multisubstituted Phosphine and Ammonia (kcal/mol) and the Optimal P···N Distance (Å)

phosphine	ΔE_{def}	ΔE_{HL}	ΔE_{pol}	ΔE_{ct}	ΔE_c	ΔE_b	R_{PN}
FH_2P	1.13	0.91	−2.62	−4.87	−0.92	−6.37	2.624
F_2PH	1.53	0.33	−2.28	−4.07	−1.01	−5.48	2.697
F_3P	1.60	0.19	−1.88	−3.19	−1.08	−4.35	2.780
$ClPH_2$	0.92	0.78	−2.34	−4.18	−0.92	−5.73	2.694
Cl_2PH	1.16	1.19	−2.37	−3.84	−1.11	−4.95	2.748
Cl_3P	1.33	2.50	−2.46	−3.89	−1.29	−3.77	2.769
CNH_2P	0.25	−2.06	−1.06	−1.33	−0.81	−5.00	2.988
$(CN)_2PH$	0.57	−2.17	−2.10	−2.88	−1.28	−7.83	2.860
$(CN)_3P$	0.64	−0.86	−3.46	−5.16	−1.68	−10.47	2.735

dx.doi.org/10.1021/jp500775m | J. Phys. Chem. A 2014, 118, 8911–8921

Table 4. Orbital Energies of the HOMO and LUMO (hartree) and the HOMO−LUMO Gaps (eV) for the Complexes of Multisubstituted Phosphines with Ammonia

	BLW			DFT		
phosphine	HOMO	LUMO	gap	HOMO	LUMO	gap
FH_2P	−0.389	0.091	13.06	−0.395	0.099	13.44
F_2PH	−0.384	0.065	12.21	−0.393	0.065	12.46
F_3P	−0.379	0.087	12.68	−0.418	0.109	14.34
$ClPH_2$	−0.388	0.063	12.27	−0.417	0.069	13.22
Cl_2PH	−0.383	0.022	11.02	−0.403	0.049	12.30
Cl_3P	−0.379	0.017	10.78	−0.404	0.040	12.08
$CNPH_2$	−0.384	0.069	12.33	−0.388	0.077	12.65
$(CN)_2PH$	−0.394	0.033	11.62	−0.403	0.035	11.92
$(CN)_3P$	−0.405	−0.006	10.86	−0.421	−0.002	11.40

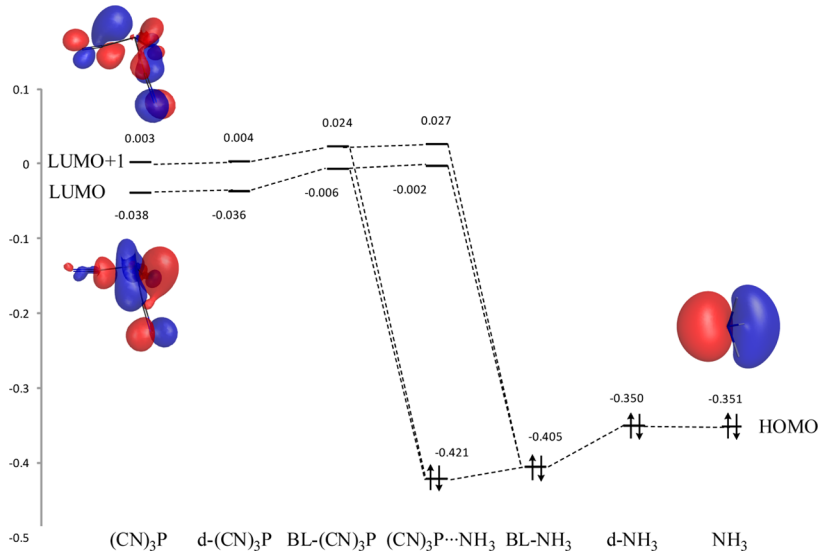

Figure 10. Molecular orbit energy change (in hartree) and the orbital correlation diagram in the formation of the $(CN)_3P\cdots NH_3$ complex, where d- and BL- denote the deformed and block-localized monomers at the geometries of the optimal complex.

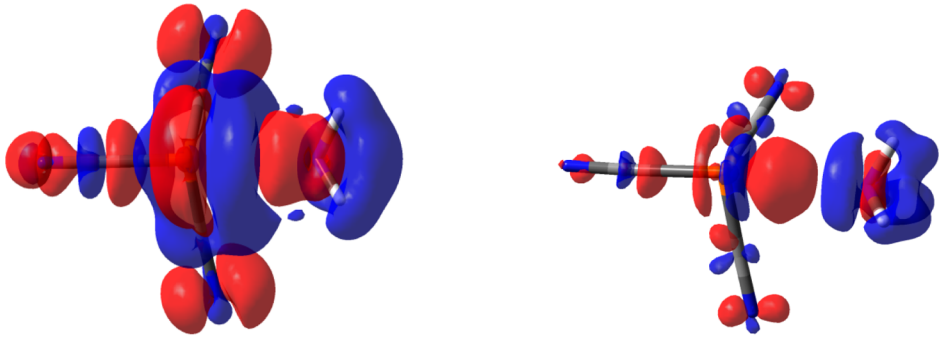

Figure 11. Electron density difference maps showing (a) polarization and (b) electron transfer in the $(CN)_3P\cdots NH_3$ complex (contour isodensity value 0.0004 au). Red/blue colors refer to the gain/loss of electron densities.

is associated with the LUMO, which is the dπ* orbital rather than the σ*(NP) orbital, we may assume that the increasing acidity of $(CN)_nPH_{3-n}$ with n is once again related to the π orbitals on the cyano groups. Indeed, the correlation diagram for $(CN)_3P$, as shown in Figure 10, shows that the interaction among the π orbitals on three cyano groups results in both the LUMO and LUMO+1 with dπ* characteristics. In fact, the LUMO of $(CN)_3P$ is a combination of σ*(CP) with two π orbitals on the last two CN groups. Note that in $CNPH_2$, the LUMO is the dπ* orbital and the LUMO+1 is the σ*(CP) orbital. The substitution of the remaining two hydrogen atoms reverses the order of these two orbitals, due to the involvement of more π orbitals on the other cyano groups. The approach of NH_3 increases the energy levels of both the LUMO and LUMO +1, but the former is up-shifted more than the latter, leading to the narrowed energy gap between the LUMO and LUMO+1. As a consequence, both can effectively accommodate electron

dx.doi.org/10.1021/jp500775m | J. Phys. Chem. A 2014, 118, 8911−8921

densities from NH_3. This explains the extremely high electron transfer energy in the $(CN)_3P\cdots NH_3$ complex.

Parts a and b of Figure 11 show that the EDD maps of $(CN)_3P\cdots NH_3$. The polarization (Figure 11a) within phosphorus tricyanide moves the electron density from the central phosphorus to the three cyano groups, whereas the electron transfer (Figure 11b) occurs from ammonia to the phosphorus atom—once again a proof for the concept of σ-hole.

CONCLUSION

Pnicogen bond refers to the bonding between a VA group element (N, P, and As), which acts as a Lewis acid and an electron donor. In this work, we analyzed the pnicogen bonds in a set of substituted phosphines complexed with ammonia, which is the Lewis base. A general belief for hydrogen bonds is that the electrostatic attraction plays the primary role, but our BLW energy decomposition analyses of the pnicogen bonds show that the orbital interaction, which involves both the polarization and electron transfer, dominates the binding. Orbital correlation diagrams are plotted to assist the understanding of the electron transfer from ammonia to substituted phosphines, which is more pronounced than the polarization effect. By examining the orbital correlations, we identify a kind of new electron transfer pathway (n $\rightarrow$ dπ* hyperconjugation) when the substituents are nitro or cyano, apart from the well-recognized n $\rightarrow$ σ*(XP) hyperconjugative interaction. In most monosubstituted phosphines XPH_2, σ*(XP) is the LUMO, which accepts electrons from the HOMO of ammonia, i.e., the lone pair on nitrogen. But for nitrophosphine and phosphinous cyanide, the LUMO is the dπ*, which results from the interaction between the π orbital of cyano or nitro substituent and the d orbital on P, and σ*(XP) becomes the LUMO+1. The strong electron transfer is in accord with the high degree of anisotropy of the pnicogen bond.

Interestingly, within the BLW method the orbital interaction can be decomposed into the polarization and electron transfer effects, which can be quantified and visualized using the electron density difference (EDD) maps separately. Although the overall orbital interaction can be well described with the interaction of a single pair of orbitals such as n $\rightarrow$ σ*(XP), EDD maps corresponding to the polarization and the electron transfer interaction reveal that this description may be overly simplified. It shows that ammonia polarizes the electron density within a substituted phosphine from the phosphorus to the substituent group side and thus enhances the bonds with P, but the electron transfer nevertheless occurs from the ammonia (mostly the lone pair on N but also hydrogen atoms) mostly to the region around P but in the opposite direction of the X−P bond. This electron transfer picture is consistent with the σ-hole theory.[41,48]

ASSOCIATED CONTENT

Supporting Information

Molecular geometries at the MP2/aug-cc-pVDZ level. Pnicogen bond lengths, bond angles, and bonding energies at both the MP2 and DFT(wB97x-D) levels are also tabulated and compared. This material is available free of charge via the Internet at http://pubs.acs.org.

AUTHOR INFORMATION

Corresponding Author

*Y. Mo: e-mail, yirong.mo@wmich.edu; phone, 269-387-2916.

Notes

The authors declare no competing financial interest.

ACKNOWLEDGMENTS

This work was supported by the US National Science Foundation under Grants CHE-1055310 and CNS-1126438.

REFERENCES

(1) Stone, A. J. *The Theory of Intermolecular Forces*; Clarendon Press: Oxford, U.K., 1996.
(2) Hobza, P.; Müller-Dethlefs, K. *Non-covalent Interactions: Theory and Experiment*; Royal Society of Chemistry: London, 2009.
(3) Lehn, J.-M. Toward Self-Organization and Complex Matter. *Science* **2002**, *295*, 2400−2403.
(4) Leckband, D.; Israelachvili, J. Intermolecular Forces in Biology. *Q. Rev. Biophys.* **2001**, *34*, 105−267.
(5) Cordier, P.; Tournilhac, F.; Soulić-Ziakovic, C.; Leibler, L. Self-Healing and Thermoreversible Rubber from Supramolecular Assembly. *Nature* **2008**, *451*, 977−980.
(6) Whitesides, G. M.; Mathias, J. P.; Seto, C. T. Molecular Self-Assembly and Nanochemistry: A Chemical Strategy for the Synthesis of Nanostructures. *Science* **1991**, *254*, 1312−1319.
(7) Stupp, S. I.; LeBonheur, V.; Walker, K.; Li, L. S.; Huggins, K. E.; Keser, M.; Amstutz, A. Supramolecular Materials: Self-Organized Nanostructures. *Science* **1997**, *276*, 384−389.
(8) Gilli, G.; Gilli, P. *The Nature of the Hydrogen Bond: Outline of a Comprehensive Hydrogen Bond Theory*; Oxford University Press: New York, 2009; Vol. 23.
(9) *Hydrogen Bonding - New Insights*; Grabowski, S. J., Ed.; Springer: Berlin, 2006; Vol. 3.
(10) Marechal, Y. *The Hydrogen Bond and the Water Molecule: The Physics and Chemistry of Water, Aqueous and Bio-Media*; Elsevier Science: Amsterdam, 2007.
(11) Nishio, M.; Hirota, M.; Umezawa, Y. *The CH/ Interaction. Evidence, Nature, and Consequences*; Wiley-VCH: New York, 1998.
(12) Desiraju, G. R.; Steiner, T. *The Weak Hydrogen Bond: In Structural Chemistry and Biology (International Union of Crystallography Monographs on Crystallography)*; Oxford University Press: New York, 2001.
(13) Jeffrey, G. A. *An Introduction to Hydrogen Bonding*; Oxford University Press: New York, 1997.
(14) Scheiner, S. *Hydrogen Bonding: A Theoretical Perspective*; Oxford University Press: New York, 1997.
(15) Pauling, L. C. *The Nature of the Chemical Bond*; 3rd ed.; Cornell University Press: Ithaca, NY, 1960.
(16) Morokuma, K. Why Do Molecules Interact? The Origin of Electron Donor-Acceptor Complexes, Hydrogen Bonding and Proton Affinity. *Acc. Chem. Res.* **1977**, *10*, 294−300.
(17) Isaacs, E. D.; Shukla, A.; Platzman, P. M.; Hamann, D. R.; Barbiellini, B.; Tulk, C. A. Covalency of the Hydrogen Bond in Ice: A Direct X-Ray Measurement. *Phys. Rev. Lett.* **1999**, *82*, 600−603.
(18) Tapan, K. G.; Viktor, N. S.; Patrick, R. K.; Ernest, R. D. Is the Hydrogen Bond in Water Dimer and Ice Covalent? *J. Am. Chem. Soc.* **2000**, *122*, 1210−1214.
(19) Grabowski, S. J. What Is the Covalency of Hydrogen Bonding? *Chem. Rev.* **2011**, *111*, 2597−2625.
(20) Gordon, M. S.; Jensen, J. H. Understanding the Hydrogen Bond Using Quantum Chemistry. *Acc. Chem. Res.* **1996**, *29*, 536−543.
(21) Liu, S. Y.; Dykstra, C. E. A Theory of Vibrational Transition Frequency Shifts Due To Hydrogen Bonding. *J. Phys. Chem.* **1986**, *90*, 3097−3103.
(22) Kollman, P. A.; Allen, L. C. Theory of the Hydrogen Bond. *Chem. Rev.* **1972**, *72*, 283−303.
(23) Guerra, C. F.; Bickelhaupt, F. M.; Baerends, E. J. Hydrogen Bonding in Mimics of Watson-Crick Base Pairs Involving C-H Proton Donor and F Proton Acceptor Groups: a Theoretical Study. *ChemPhysChem* **2004**, *5*, 481−487.

(24) Trudeau, G. T.; Dumas, J. M.; Dupuis, P.; Guerin, M.; Sandorfy, C. Intermolecular Interactions and Anesthesia: Infrared Spectroscopic Studies. *Top. Curr. Chem.* **1980**, *93*, 91−125.
(25) Buděšínský, M.; Fiedler, P.; Arnold, Z. Triformylmethane: An Efficient Preparation, Some Derivatives, and Spectra. *Synthesis* **1989**, *1989*, 858−860.
(26) Boldeskul, I. E.; Tsymbal, I. F.; Ryltsev, E. V.; Latajka, Z.; Barnes, A. J. Reversion of the Usual ν(C-H/D) Spectral Shift of Haloforms in Some Hydrogen-Bonded Complexes. *J. Mol. Struct.* **1997**, *436*−*437*, 167−171.
(27) Hobza, P.; Špirko, V.; Selzle, H. L.; Schlag, E. W. Anti-Hydrogen Bond in the Benzene Dimer and Other Carbon Proton Donor Complexes. *J. Phys. Chem. A* **1998**, *102*, 2501−2504.
(28) Hobza, P.; Špirko, V.; Havlas, Z.; Buchhold, K.; Reimann, B.; Barth, H. D.; Brutschy, B. Anti-Hydrogen Bond Between Chloroform and Fluorobenzene. *Chem. Phys. Lett.* **1999**, *299*, 180−186.
(29) Hobza, P.; Havlas, Z. Blue-shifting Hydrogen Bonds. *Chem. Rev.* **2000**, *100*, 4253−4264.
(30) van der Veken, B. J.; Herrebout, W. A.; Szostak, R.; Shchepkin, D. N.; Havlas, Z.; Hobza, P. The Nature of Improper, Blue-Shifting Hydrogen Bonding Verified Experimentally. *J. Am. Chem. Soc.* **2001**, *123*, 12290−12293.
(31) Egli, M.; Sarkhel, S. Lone pair-aromatic interactions: To Stabilize or Not to Stabilize. *Acc. Chem. Res.* **2007**, *40*, 197−205.
(32) Wright, A. M.; Howard, A. A.; Howard, C.; Tschumper, G. S.; Hammer, N. I. Charge Transfer and Blue Shifting of Vibrational Frequencies in a Hydrogen Bond Acceptor. *J. Phys. Chem. A* **2013**, *117*, 5435−5446.
(33) Li, X. S.; Liu, L.; Schlegel, H. B. On the Physical Origin of Blue-shifted Hydrogen Bonds. *J. Am. Chem. Soc.* **2002**, *124*, 9639−9647.
(34) Alabugin, I. V.; Manoharan, M.; Peabody, S.; Weinhold, F. Electronic Basis of Improper Hydrogen Bonding: A Subtle Balance of Hyperconjugation and Rehybridization. *J. Am. Chem. Soc.* **2003**, *125*, 5973−5987.
(35) Joseph, J.; Jemmis, E. D. Red-, Blue-, or No-Shift in Hydrogen Bonds: A Unified Explanation. *J. Am. Chem. Soc.* **2007**, *129*, 4620−4632.
(36) Metrangolo, P.; Neukirch, H.; Pilati, T.; Resnati, G. Halogen Bonding Based Recognition Processes: A World Parallel to Hydrogen Bonding. *Acc. Chem. Res.* **2005**, *38*, 386−395.
(37) Metrangolo, P.; Meyer, F.; Pilati, T.; Resnati, G.; Terraneo, G. Halogen Bonding in Supramolecular Chemistry. *Angew. Chem., Int. Ed.* **2008**, *47*, 6114−6127.
(38) Priimagi, A.; Cavallo, G.; Metrangolo, P.; Resnati, G. The Halogen Bond in the Design of Functional Supramolecular Materials: Recent Advances. *Acc. Chem. Res.* **2013**, *46*, 2686−2695.
(39) Politzer, P.; Lane, P.; Concha, M. C.; Ma, Y.; Murray, J. S. An Overview of Halogen Bonding. *J. Mol. Model.* **2007**, *13*, 305−311.
(40) Auffinger, P.; Hays, F. A.; Westhof, E.; Ho, P. S. Halogen Bonds in Biological Molecules. *Proc. Natl. Acad. Sci.* **2004**, *101*, 16789−16794.
(41) Clark, T.; Hennemann, M.; Murray, J. S.; Politzer, P. Halogen Bonding: the σ-Hole. *J. Mol. Model.* **2007**, *13*, 293−296.
(42) Wang, W.; Ji, B.; Zhang, Y. Chalcogen bond: A Sister Noncovalent Bond to Halogen Bond. *J. Phys. Chem. A* **2008**, *113*, 8232−8135.
(43) Syzgantseva, O. A.; Tognetti, V.; Joubert, L. On the Physical Nature of Halogen Bonds: A QTAIM Study. *J. Phys. Chem. A* **2013**, *117*, 8969−8980.
(44) Sanz, P.; Yáñez, M.; Mó, O. Competition between X···H···Y Intramolecular Hydrogen Bonds and X···Y (X = O, S, and Y = Se, Te) Chalcogen−Chalcogen Interactions. *J. Phys. Chem. A* **2002**, *106*, 4661−4668.
(45) Iwaoka, M.; Takemoto, S.; Tomoda, S. Statistical and Theoretical Investigations on the Directionality of Nonbonded S···O Interactions. Implications for Molecular Design and Protein Engineering. *J. Am. Chem. Soc.* **2002**, *124*, 10613−10620.
(46) Werz, D. B.; Gleiter, R.; Rominger, F. Nanotube Formation Favored by Chalcogen−Chalcogen Interactions. *J. Am. Chem. Soc.* **2002**, *124*, 10638−10639.
(47) Bleiholder, C.; Werz, D. B.; Köppel, H.; Gleiter, R. Theoretical Investigations on Chalcogen−Chalcogen Interactions: What Makes These Nonbonded Interactions Bonding? *J. Am. Chem. Soc.* **2006**, *128*, 2666−2674.
(48) Clark, T. σ-Holes. *WIREs Comput. Mol. Sci.* **2013**, *3*, 13−20.
(49) Politzer, P.; Murray, J. S.; Clark, T. Halogen Bonding and Other σ-Hole Interactions: A Perspective. *Phys. Chem. Chem. Phys.* **2013**, *15*, 11178−11189.
(50) Philp, D.; Stoddart, J. F. Self-Assembly in Natural and Unnatural Systems. *Angew. Chem., Int. Ed.* **1996**, *35*, 1154−1196.
(51) Scheiner, S. The Pnicogen Bond: Its Relation to Hydrogen, Halogen, and Other Noncovalent Bonds. *Acc. Chem. Res.* **2013**, *46*, 280−288.
(52) Zahn, S.; Frank, Z.; Hey-Hawkins, E.; Kirchner, B. Pnicogen Bonds: A New Molecular Linker? *Chem.—Eur. J.* **2011**, *17*, 6034−6038.
(53) Del Bene, J. E.; Alkorta, I.; Sánchez-Sanz, G.; Elguero, J. Phosphorus As a Simultaneous Electron-Pair Acceptor in Intermolecular P···N Pnicogen Bonds and Electron-Pair Donor to Lewis Acids. *J. Phys. Chem. A* **2013**, *117*, 3133−3141.
(54) Bauer, S.; Tschirschwitz, S.; Lönnecke, P.; Frank, R.; Kirchner, B.; Clarke, M. L.; Hey-Hawkins, E. Enantiomerically Pure Bis-Phosphonito Carbaborane(12) Compounds. *Eur. J. Inorg. Chem.* **2009**, *2009*, 2776−2788.
(55) Watt, M. M.; Collins, M. S.; Johnson, D. W. Ion-π Interactions in Ligand Design for Anions and Main Group Cations. *Acc. Chem. Res.* **2013**, *46*, 955−966.
(56) Bauzá, A.; Quiñonero, D.; Deyà, P. M.; Frontera, A. Pnicogen−π Complexes: Theoretical study and biological implications. *Phys. Chem. Chem. Phys.* **2012**, *14*, 14061−14066.
(57) Moilanen, J.; Ganesamoorthy, C.; Balakrishna, M. S.; Tuononen, H. M. Weak Interactions Between Trivalent Pnictogen Centers: Computational Analysis of Bonding in Dimers $X_3E\cdots EX_3$ (E = Pnictogen, X = Halogen). *Inorg. Chem.* **2009**, *48*, 6740−6747.
(58) Scheiner, S. A New Noncovalent Force: Comparison of P···N Interaction with Hydrogen and Halogen Bonds. *J. Chem. Phys.* **2011**, *134*, 094315.
(59) Del Bene, J. E.; Alkorta, I.; Sanchez-Sanz, G.; Elguero, J. Structures, Energies, Bonding, and NMR Properties of Pnicogen Complexes $H_2XP{:}NXH_2$ (X = H, CH_3, NH_2, OH, F, Cl). *J. Phys. Chem. A* **2011**, *115*, 13724−13731.
(60) Bauza, A.; Quinonero, D.; Deya, P. M.; Frontera, A. Pnicogen-π Complexes: Theoretical Study and Biological Implications. *Phys. Chem. Chem. Phys.* **2012**, *14*, 14061−14066.
(61) Li, Q. Z.; Li, R.; Liu, X. F.; Li, W. Z.; Cheng, J. B. Pnicogen-Hydride Interaction Between FH_2X (X = P and As) and HM (M = ZnH, BeH, MgH, Li, and Na). *J. Phys. Chem. A* **2012**, *116*, 2547−2553.
(62) Adhikari, U.; Scheiner, S. Sensitivity of Pnicogen, Chalcogen, Halogen and H-Bonds to Angular Distortions. *Chem. Phys. Lett.* **2012**, *532*, 31−35.
(63) Alkorta, I.; Sanchez-Sanz, G.; Elguero, J. Influence of Hydrogen Bonds on the P···P Pnicogen Bond. *J. Chem. Theory Comput.* **2012**, *8*, 2320−2327.
(64) An, X. L.; Li, R.; Li, Q. Z.; Liu, X. F.; Li, W. Z.; Cheng, J. B. Substitution, Cooperative, and Solvent Effects on π Pnicogen Bonds in the FH_2P and FH_2As Complexes. *J. Mol. Model.* **2012**, *18*, 4325−4332.
(65) Del Bene, J. E.; Alkorta, I.; Sanchez-Sanz, G.; Elguero, J. Interplay of F-H···F Hydrogen Bonds and P···N Pnicogen Bonds. *J. Phys. Chem. A* **2012**, *116*, 9205−9213.
(66) Scheiner, S. Detailed Comparison of the Pnicogen Bond with Chalcogen, Halogen, and Hydrogen Bonds. *Int. J. Quantum Chem.* **2013**, *113*, 1609−1620.
(67) Alkorta, I.; Elguero, J.; Del Bene, J. E. Pnicogen-Bonded Cyclic Trimers $(PH_2X)_3$ with X = F, Cl, OH, NC, CN, CH_3, H, and BH_2. *J. Phys. Chem. A* **2013**, *117*, 4981−4987.

(68) Solimannejad, M.; Gholipour, A. Revealing Substituent Effects on the Concerted Interaction of Pnicogen, Chalcogen, and Halogen Bonds in Substituted σ-Triazine Ring. *Struct. Chem.* **2013**, *24*, 1705−1711.
(69) Alkorta, I.; Elguero, J.; Del Bene, J. E. Pnicogen Bonded Complexes of PO_2X (X = F, Cl) with Nitrogen Bases. *J. Phys. Chem. A* **2013**, *117*, 10497−10503.
(70) Del Bene, J. E.; Alkorta, I.; Elguero, J. Properties of complexes H2C=(X)P:PXH2, for X = F, Cl, OH, CN, NC, CCH, H, CH3, and BH2: P···P Pnicogen Bonding at σ-Holes and π-Holes. *J. Phys. Chem. A* **2013**, *117*, 11592−11604.
(71) Eskandari, K.; Mahmoodabadi, N. Pnicogen Bonds: A theoretical Study Based on the Laplacian of Electron Density. *J. Phys. Chem. A* **2013**, *117*, 13018−13024.
(72) Scheiner, S. Effects of Substituents Upon the P···N Noncovalent Interaction: The Limits of Its Strength. *J. Phys. Chem. A* **2011**, *115*, 11202−11209.
(73) Mohajeri, A.; Pakiari, A. H.; Bagheri, N. Theoretical Studies on the Nature of Bonding in σ-Hole Complexes. *Chem. Phys. Lett.* **2009**, *467*, 393−397.
(74) Del Bene, J. E.; Alkorta, I.; Elguero, J. Characterizing Complexes with Pnicogen Bonds Involving sp^2 Hybridized Phosphorus Atoms: $(H_2C{=}PX)_2$ with X = F, Cl, OH, CN, NC, CCH, H, CH_3, and BH_2. *J. Phys. Chem. A* **2013**, *117*, 6893−6903.
(75) Mo, Y. Geometrical Optimization for Strictly Localized Structures. *J. Chem. Phys.* **2003**, *119*, 1300−1306.
(76) Mo, Y.; Peyerimhoff, S. D. Theoretical Analysis of Electronic Delocalization. *J. Chem. Phys.* **1998**, *109*, 1687−1697.
(77) Mo, Y.; Song, L.; Lin, Y. The block-localized Wavefunction (BLW) Method At the Density Functional Theory (DFT) Level. *J. Phys. Chem. A* **2007**, *111*, 8291−8301.
(78) Mo, Y.; Bao, P.; Gao, J. Energy Decomposition Analysis Based on a Block-Localized Wavefunction and Multistate Density Functional Theory. *Phys. Chem. Chem. Phys.* **2011**, *13*, 6760−6775.
(79) Mo, Y.; Gao, J.; Peyerimhoff, S. D. Energy Decomposition Analysis of Intermolecular Interactions Using a Block-Localized Wavefunction Approach. *J. Chem. Phys.* **2000**, *112*, 5530−5538.
(80) *Valence Bond Theory*; Cooper, D. L., Ed.; Elsevier: Amsterdam, 2002.
(81) Gallup, G. A. *Valence Bond Methods: Theory and Applications*; Cambridge University Press: New York, 2002.
(82) Shaik, S. S.; Hiberty, P. C. *A Chemist's Guide to Valence Bond Theory*; Wiley: Hoboken, NJ, 2008.
(83) Wu, W.; Su, P.; Shaik, S.; Hiberty, P. C. Classical Valence Bond Approach by Modern Methods. *Chem. Rev.* **2011**, *111*, 7557−7593.
(84) Stoll, H.; Preuss, H. On the Direct Calculation of Localized HF Orbitals in Molecule Clusters, Layers and Solids. *Theor. Chim. Acta* **1977**, *46*, 11−21.
(85) Stoll, H.; Wagenblast, G.; Preuss, H. On the Use of Local Basis Sets for Localized Molecular Orbitals. *Theor. Chim. Acta* **1980**, *57*, 169−178.
(86) Mehler, E. L. Self-Consistent, Nonorthogonal Group Function Approximation for Polyatomic systems. I. Closed Shells. *J. Chem. Phys.* **1977**, *67*, 2728−2739.
(87) Mehler, E. L. Self-Consistent, Nonorthogonal Group Function Approximation for Polyatomic Systems. II. Analysis of Noncovalent Interactions. *J. Chem. Phys.* **1981**, *74*, 6298−6306.
(88) Gianinetti, E.; Raimondi, M.; Tornaghi, E. Modification of the Roothaan Equations to Exclude BSSE from Molecular Interaction Calculations. *Int. J. Quantum Chem.* **1996**, *60*, 157−166.
(89) Famulari, A.; Gianinetti, E.; Raimondi, M.; Sironi, M. Implementation of Gradient-Optimization Algorithm and Force Constant Computatins in BSSE-Free Direct and Conventional SCF Approaches. *Int. J. Quantum Chem.* **1998**, *69*, 151−158.
(90) Khaliullin, R. Z.; Cobar, E. A.; Lochan, R. C.; Bell, A. T.; Head-Gordon, M. Unravelling the Origin of Intermolecular Interactions Using Absolutely Localized Molecular Orbitals. *J. Phys. Chem. A* **2007**, *111*, 8753−8765.
(91) Kitaura, K.; Morokuma, K. A New Energy Decomposition Scheme for Molecular Interactions within the Hartree-Fock Approximation. *Int. J. Quantum Chem.* **1976**, *10*, 325−340.
(92) Ziegler, T.; Rauk, A. On the Calculation of Bonding Energies by the Hartree Fock Slater Method. *Theor. Chem. Acc.* **1977**, *46*, 1−10.
(93) Bagus, P. S.; Hermann, K.; Bauschlicher, C. W., Jr. A New Analysis of Charge Transfer and Polarization for Ligand-Metal Bonding: Model Studies of Carbonylaluminum (Al_4CO) and Ammineraluminum (Al_4NH_3). *J. Chem. Phys.* **1984**, *80*, 4378−4386.
(94) Stevens, W. J.; Fink, W. H. Frozen Fragment Reduced Variational Space Analysis of Hydrogen Bonding Interactions. Application to the Water Dimer. *Chem. Phys. Lett.* **1987**, *139*, 15−22.
(95) Glendening, E. D.; Streitwieser, A. Natural Energy Decomposition Analysis - An Energy Partitioning Procedure for Molecular-Interactions with Application to Weak Hydrogen-Bonding, Strong Ionic, and Moderate Donor-Acceptor Interactions. *J. Chem. Phys.* **1994**, *100*, 2900−2909.
(96) Chen, W.; Gordon, M. S. Energy Decomposition Analyses for Many-Body Interaction and Applications to Water Complexes. *J. Phys. Chem.* **1996**, *100*, 14316−14328.
(97) van der Vaart, A.; Merz, K. M., Jr. Divide and Conquer Interaction Energy Decomposition. *J. Phys. Chem. A* **1999**, *103*, 3321−3329.
(98) Reinhardt, P.; Piquemal, J.-P.; Savin, A. Fragment-Localized Kohn−Sham Orbitals via a Singles Configuration-Interaction Procedure and Application to Local Properties and Intermolecular Energy Decomposition Analysis. *J. Chem. Theory Comput.* **2008**, *4*, 2020−2029.
(99) Wu, Q.; Ayers, P. W.; Zhang, Y. K. Density-Based Energy Decomposition Analysis for Intermolecular Interactions with Variationally Determined Intermediate State Energies. *J. Chem. Phys.* **2009**, *131*, 164112.
(100) Su, P.; Li, H. Energy Decomposition Analysis of Covalent Bonds and Intermolecular Interactions. *J. Chem. Phys.* **2009**, *131*, 014101.
(101) Bickelhaupt, F. M.; Baerends, E. J. In *Reviews in Computational Chemistry*; Lipkowitz, K. B., Boyd, D. B., Eds.; Wiley-VCH: New York, 1999; Vol. *15*, p 1.
(102) Lein, M.; Szabo, A.; Kovacs, A.; Frenking, G. Theoretical Studies of Inorganic Compounds. Part XXVIII. Energy Decomposition Analysis of the Chemical Bond in Main Group and Transition metal Compounds. *Faraday Discuss.* **2003**, *124*, 365−378.
(103) Erhardt, S.; Frenking, G. A Challenge to Chemical Intuition: Donor-Acceptor Interactions in H_3B-L and H_2B^+-L (L = CO; EC_5H_5, E =N-Bi). *Chem.—Eur. J.* **2006**, *12*, 4620−4629.
(104) Steinmann, S. N.; Corminboeuf, C.; Wu, W.; Mo, Y. Dispersion-Corrected Energy Decomposition Analysis for Intermolecular Interactions Based on the BLW and dDXDM Methods. *J. Phys. Chem. A* **2011**, *115*, 5467−5477.
(105) Schmidt, M. W.; Baldridge, K. K.; Boatz, J. A.; Elbert, S. T.; Gordon, M. S.; Jensen, J. J.; Koseki, S.; Matsunaga, N.; Nguyen, K. A.; Su, S.; et al. General Atomic and Molecular Electronic Structure System. *J. Comput. Chem.* **1993**, *14*, 1347−1363.
(106) Grimme, S. Semiempirical GGA-type Density Functional Constructed with a Long-Range Dispersion Correction. *J. Comput. Chem.* **2006**, *27*, 1787−1799.
(107) McConnell, H. Intramolecular Charge Transfer in Aromatic Free Radicals. *J. Chem. Phys.* **1961**, *35*, 508−515.
(108) Mo, Y.; Song, L.; Liu, M.; Lin, Y.; Cao, Z.; Wu, W. Block-Localized Wavefunction (BLW) Based Two-State Approach for Charge Transfers between Phenyl Rings. *J. Chem. Theory Comput.* **2012**, *8*, 800−805.
(109) Mo, Y.; Wu, W.; Q, Z. Study of Intramolecular Electron Transfer with a Two-State Model Based on the Orbital Deletion Procedure. *J. Chem. Phys.* **2003**, *119*, 6448−6456.